Comparison of the Ablation Behavior of Polymer Films in the IR and UV with Nanosecond and Picosecond Pulses

Ch. Hahn,[†] T. Lippert,[‡] and A. Wokaun*[,†,§]

General Energy Research, Paul Scherrer Institute, CH-5232 Villigen PSI, Switzerland, Department of Chemical Engineering and Industrial Chemistry, Swiss Federal Institute of Technology, CH-8092 Zurich, Switzerland, and Division of Chemical Science and Technology, Los Alamos National Laboratory, Los Alamos, MS J585, New Mexico 87545

Received: September 3, 1998; In Final Form: December 17, 1998

Experiments are performed to compare the ablation behavior in the IR and UV spectral regions of a doped standard polymer, PMMA, and a specially tailored photopolymer, i.e., a triazene copolyester, to elucidate the underlying mechanisms. The results are discussed in light of current theories about photochemical and photothermal pathways of ablation. Further experiments are performed with nanosecond and picosecond pulses to study the impact of pulse length on the material. From the failure to induce ablation in the IR by doping the specialty polymer with an optical molecular heater we conclude that etching in the UV of this compound is mainly governed by a photochemical process. This result is contrasted by successful ablation of doped PMMA in the IR via a thermal unzipping mechanism. With respect to practical applications, the results show convincingly that the presence of an absorbing chromophore in the polymer is a prerequisite for achieving high-resolution structuring, since molecular absorption is required for an efficient distribution of incorporated photonic energy.

Introduction

Excimer laser ablation lithography (EAL) is now a widely used technique for microstructuring. One of the main advantages is the so-called "dry-etching" capability, which implies that no additional wet-developing steps are necessary after irradiation; in addition, the resist removal can be performed under air. This means a reduction of costs and thus makes the technique attractive for industrial applications, e.g., for thin film transistor−liquid crystal display (TFT−LCD) manufacturing.[1] A further step in the reduction of costs would be the use of solid-state lasers instead of excimer lasers, especially if the fundamental wavelength can be used.

Despite the practical implementations, there is still a debate about the underlying mechanism of doped polymer ablation, i.e., photothermal[2−4] vs photochemical[5−7] pathways. In the photothermal mechanism the dopant acts as a molecular optical heating element; after absorption of photons, the energy is released to the polymer matrix via vibrational cooling. Thus, a rapid temperature increase is induced in the bulk material, leading to a thermal decomposition of the polymer and eventually to ablation if there is sufficient energy left for the fragments to leave the matrix. In contrast, in the photochemical mechanism, the absorbed photonic energy leads to photodecomposition of the dopant molecule, yielding gaseous photoproducts. The instant volume increase exerts high pressure on the surrounding polymer, resulting in ablation.

In this study we investigated the ablation behavior of doped material in the IR (1064 nm) and the UV (266 nm) regions in order to separate photochemical and photothermal parts of the ablation mechanism. For materials, we chose a technically relevant polymer, PMMA, and a specialty polymer tailored for ablation in the UV, a triazene-containing copolyester. A dye named IR-165 is used as a molecular point heater as described above for the experiments at 1064 nm.[8] Diazo Meldrum's acid (DMA), which is a well-known photoactive molecule, is suggested for use as a positive photoresist applying deep UV irradiation[9] and was used before in dopant-induced ablation at 248 nm.[10] In the specialty polymer, the photoactive group, i.e., a triazene chromophore, is incorporated directly in the main chain. The advantage, compared to monomer-doped systems, is the optimum deposition of energy into the bulk material. For the latter approach, the minor quality of etched patterns reported in the literature has been attributed mainly to the preferential ablation of the dopant.

We also performed experiments with different pulse lengths (picosecond vs nanosecond) to elucidate the impact of intensity on the ablation mechanism, thus enabling the etching of otherwise transparent polymers or materials that have a high thermal conductivity, such as metals.

Experimental Section

Material. The PMMA samples were ca. 13 μm thick and doped with either diazo Meldrum's acid (DMA, TCI America; Chart 1, left) or IR-165 (American Cyanamid, Woodbury, NY 11797; Chart 1, right). The samples were prepared by dissolving the appropriate amount of components (750 mg PMMA (Aldrich, M_w = 120 000), 140 mg IR-165, and/or 210 mg of DMA) in 15 mL of tetrahydrofuran and were cast from solution using draw bars on polypropylene sheets. The dopant is indicated in the designation of the samples: PMMA-IR is doped with IR-165, PMMA-IR/UV is doped with both, and PMMA-UV is doped with DMA.

The triazene copolyester films are about 20 μm thick and solvent cast on a glass substrate. The structure of the specialty polymers is shown in Chart 2; the synthesis has been described

[†] Paul Scherrer Institute.
[‡] Los Alamos National Laboratory.
[§] Swiss Federal Institute of Technology.

10.1021/jp983609j CCC: $18.00
Published on Web 02/06/1999

CHART 1: Chemical Structure of the Dopants Diazo Meldrum's Acid (Left) and IR-165 (Right)

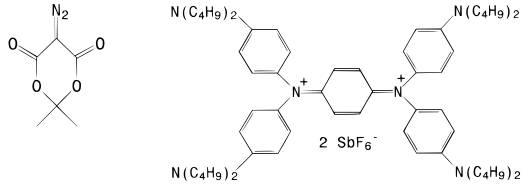

elsewhere.[11] The triazene content (m) is indicated in the name as a percentage {$=100m/(m + n)$}; e.g., CP35 signifies a copolymer synthesized with 35% triazene containing diol and 65% of a competing monomer with benzylic hydroxy groups (Chart 2). CP100-IR was additionally doped with 20 wt % of IR-165 for irradiation experiments at 1064 nm.

Ablation Procedure. For the nanosecond ablation experiments a Nd:YAG (Continuum) was used (1064 nm, 8 ns) quadrupled for UV pulses (266 nm, 6 ns) at a repetition rate of 10 Hz. Pulses in the picosecond regime are generated from the fundamental wavelength of a picosecond mode-locked Nd:YAG (Coherent Antares), which is used to seed a regenerative amplifier (home-built) at a repetition rate of 50 Hz. The resulting pulse lengths are 100 ps at 1064 nm and 60 ps at 266 nm. By use of an optical chopper, a repetition rate of 25 Hz was chosen for sample irradiation. The samples were mounted on computerized stages, which were moved concertedly with the pulse repetition (10 and 25 Hz) to achieve single-pulse irradiation at any given sample position unless noted otherwise. The beam outputs were focused onto the sample surface using a 25 mm CaF_2 lens. The laser power was varied by using an attenuator. To account for the pulse-to-pulse variation of the energy, all determined ablation depth values are averaged over several sample positions and error bars are given in the graphs. The ablated depth was determined by a surface profiler (DekTak 8000).

Compared to experiments with excimer lasers, which excel by a flat-top energy profile, craters from a Nd:YAG laser with its Gaussian energy distribution (in the ideal case) are much more complicated to evaluate with respect to the etch depth. Since the Nd:YAG lasers used for this investigation exhibited a very inhomogeneous energy distribution, we decided to take the mean value of the detected depth profile. The irradiated surface area was investigated with scanning electron microscopy (Topcon ABT60).

Results

Triazene Copolyesters CP35 and CP50. Irradiation at 266 nm (with Picosecond and Nanosecond Pulses). Two samples of the copolyesters with 30% and 50% triazene content were irradiated with 266 nm at both pulse lengths. In Figure 1 the UV−vis spectrum of CP50 is shown. Clean ablation was achieved for both polymers and both picosecond and nanosecond pulse lengths. The SEM picture (Figure 2) shows the edges of craters after single-pulse irradiation. Sharp contours with no redeposited material outside the craters are revealed for both

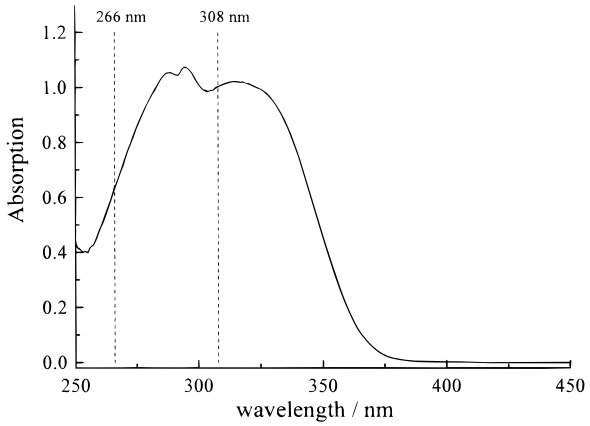

Figure 1. UV−vis spectrum of the triazene containing copolyester CP50.

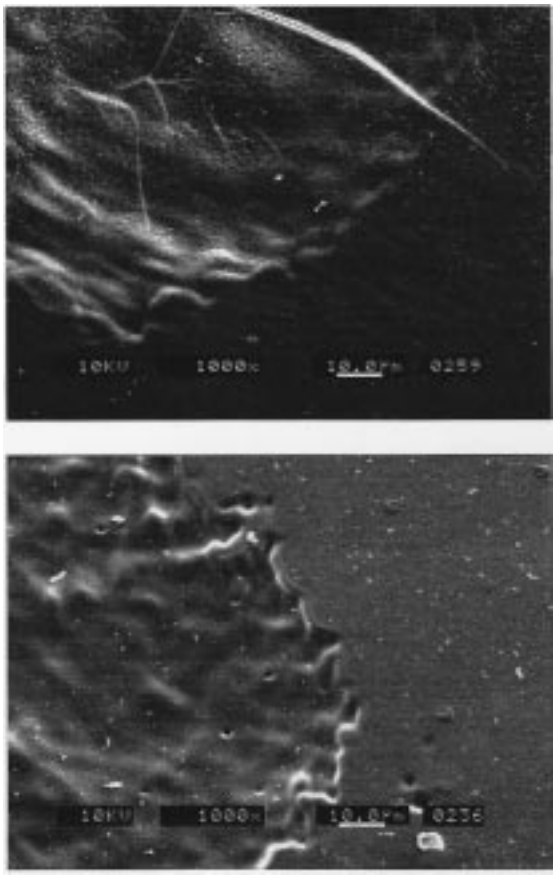

Figure 2. SEM micrograph of specialty polymers ablated at 266 nm with single pulses: (top) CP50 (480 mJ/cm^2, 60 ps); (bottom) CP35 (470 mJ/cm^2, 6 ns).

CHART 2.

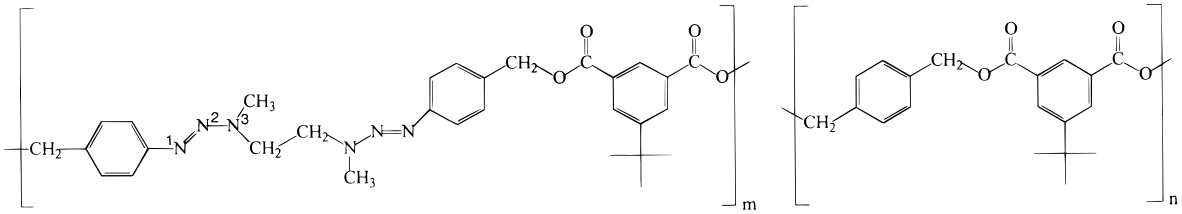

The content of triazene units {$=100m/(m + n)$} is used for identification, e.g., CP50 implies that 50% triazene-containing monomers are included in the copolymer.

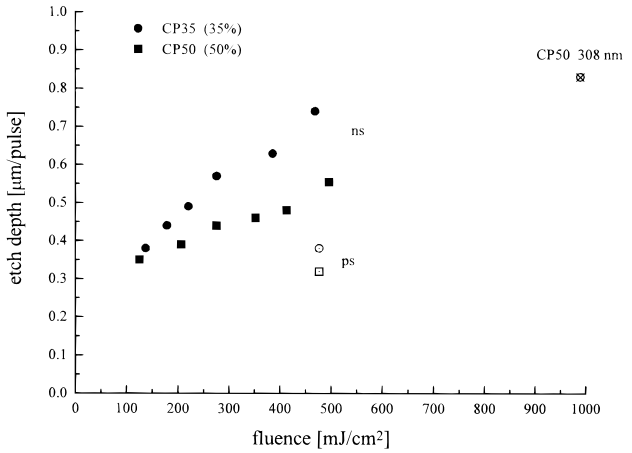

Figure 3. Etch depths as a function of the fluence for 266 nm ablation (ns) of CP35 (circles) and CP50 (squares). For comparison, values for picosecond pulses at 266 nm and nanosecond pulses at 308 nm are indicated.

pulse durations. The irregular structure is due to the beam profile of the pump pulse. Figure 3 shows the etch depths as a function of the fluence for nanosecond pulses. The ablated depth is slightly higher for the copolyester with lower triazene content, and there are indications that the threshold fluence is also higher, but owing to the lack of experimental data in that region, no final conclusion can be drawn. A rough calculation of the threshold fluence, using the thermal model[12]

$$d = \frac{1}{\alpha_{\text{eff}}} \ln \frac{F}{F_0}$$

(with d = etch depth, α_{eff} = effective absorption coefficient, F = fluence), yields effective absorption coefficients α_{eff} of 3.5 μm^{-1} (CP35) and 5.9 μm^{-1} (CP50) and threshold fluences F_0 of 37 mJ/cm^2 (CP35) and 21 mJ/cm^2 (CP50). The observation of lower ablation rates in the polymers with the higher triazene content is in accordance with the higher absorption coefficient. For irradiation with picosecond pulses a lower etch depth results in a fluence similar to that of the nanosecond experiments. One value for irradiation with 308 nm excimer laser is included in Figure 3. A comparison of the ablation parameters given above with those from experiments at 308 nm is difficult because much higher fluences were applied. But calculations according to the equation above result in higher threshold fluences (280 mJ/cm^2 for CP50).

Triazene Copolyester CP100-IR. Irradiation at 1064 nm (with Picosecond and Nanosecond Pulses). To test the possibility to structure polymers at the fundamental (1064 nm) of a Nd:YAG laser, a copolyester (transparent at 1064 nm) with 100% triazene units in the backbone was additionally doped with IR-165 to induce photothermal ablation at 1064 nm. Neither with picosecond nor with nanosecond single pulses clean etching could be achieved. In the investigated fluence range (0.1−2 J/cm^2) the material exhibits only swelling and surface roughening with both nanosecond and picosecond pulse lengths. At some irradiated areas open bubbles are found, obviously due to high pressure that exceeds the mechanical strength of the material (Figure 4). Only with multiple pulses (>50) could etching be achieved. The walls appear very porous and show thermal damage, and debris is ejected and redeposited outside the crater. The etching is probably due to thermal modification of the polymer, e.g., carbonization, which induced additional absorption sites. This is supported by the fact that a thin layer of material remains on the glass substrate, which is not removed even after many pulses.

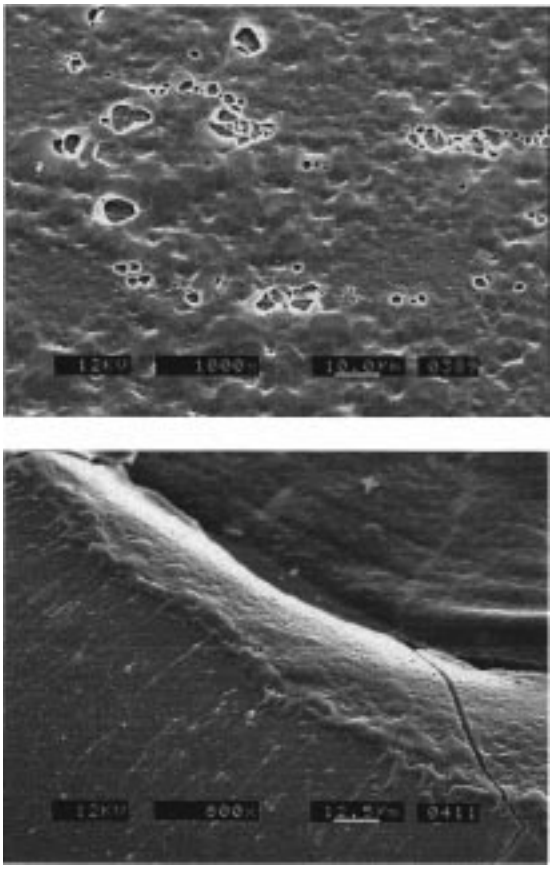

Figure 4. SEM micrographs of CP100-IR irradiated at 1064 nm (8 ns, 1.1 J/cm^2): (top) single pulse; (bottom) multiple pulses n > 50.

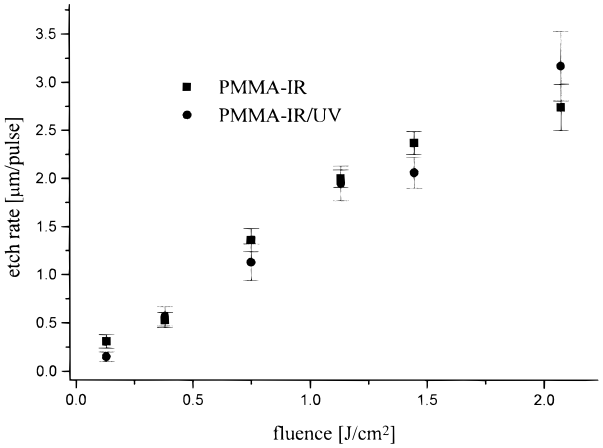

Figure 5. Comparison of the etch depths of PMMA-IR and PMMA-IR/UV after irradiation at 1064 nm, 100 ps.

PMMA-IR, PMMA-IR/UV. Irradiation at 1064 nm (with Picosecond and Nanosecond Pulses). Distinctive differences for irradiation with picosecond and nanosecond pulses are revealed in the case of doped PMMA. Although etching is achieved with picosecond pulses, the material is only partly removed with nanosecond *single pulses* for both samples (PMMA-IR and PMMA-IR/UV) in the investigated fluence range (0.1−1.1 J/cm^2). Therefore, no etch depths could be determined for nanosecond ablation. In Figure 5 a comparison of the etch rates achieved with picosecond single pulses for both samples is shown. Within the experimental errors the addition of diazo Meldrum's acid seems to have no or only a minor

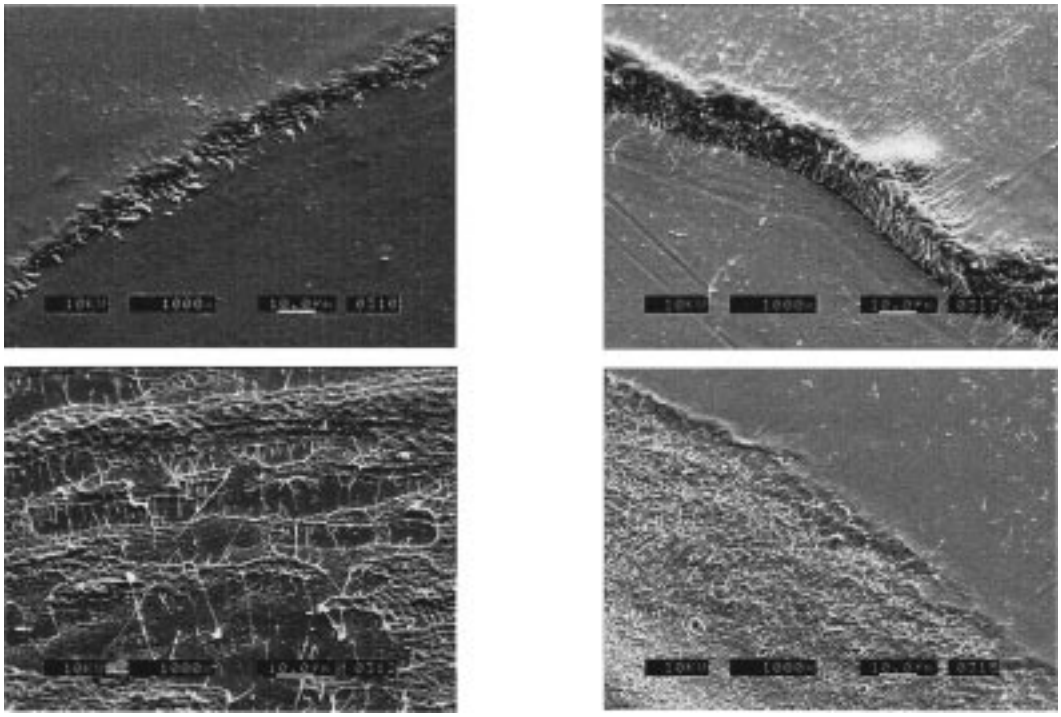

Figure 6. SEM micrographs of PMMA-IR (left) and PMMA-IR/UV (right) irradiated at 1064 nm (8 ns, 1.1 J/cm^2): (top) multiple pulses ($n > 50$); (bottom) single pulse.

influence on the ablation rates. The morphology of the ablation contours was investigated with SEM. Irradiation with nanosecond single pulses leads to surface swelling. The spongy structure of PMMA-IR/UV looks less coarse than the one of PMMA-IR (Figure 6, bottom). For the latter, parts of the irradiated area appear to be cleanly etched, while fibrous debris is deposited over other parts. *Multipulse* irradiation results in significant etching with smooth bottoms; only the walls have a foamy appearance (Figure 6, top). The removal of the foamy material with a standard PMMA developer (methyl isobutyl ketone/isopropyl alcohol, 3:1)[13] was not successful, which is probably because of the high concentration of the dopant that is soluble in methyl isobutyl ketone. Therefore, the highest concentration of methyl isobutyl ketone that could be used was 1:3, but in this mixture the irradiated material was not soluble.

The surface modifications for picosecond irradiation are quite different. Although a strong surface roughening is observed, even at the lowest investigated fluence (130 mJ/cm^2) etching can be detected with the profiler. At higher energies the bottoms appear partly smooth and partly foamy, while at the edges very fine polymer fibers are redeposited (Figure 7). A remarkable change in the morphology is observed for both samples at higher fluences; concentrical ringlike patterns are detected everywhere in the irradiated area (more than 20 equidistant rings can be counted in one pattern; Figure 8, top), while for lower fluences the spongy structure looks more netlike. The "ring-pattern" was exclusively observed after 1064 nm picosecond irradiation of these two samples in the present investigation. For multipulse irradiation a very smooth bottom is observed; only PMMA-IR/UV exhibits some ruptured bubbles, which are few in number but comparatively large (up to 100 μm; Figure 8, bottom), probably because of decomposition of DMA in the deeper layers of the polymer.

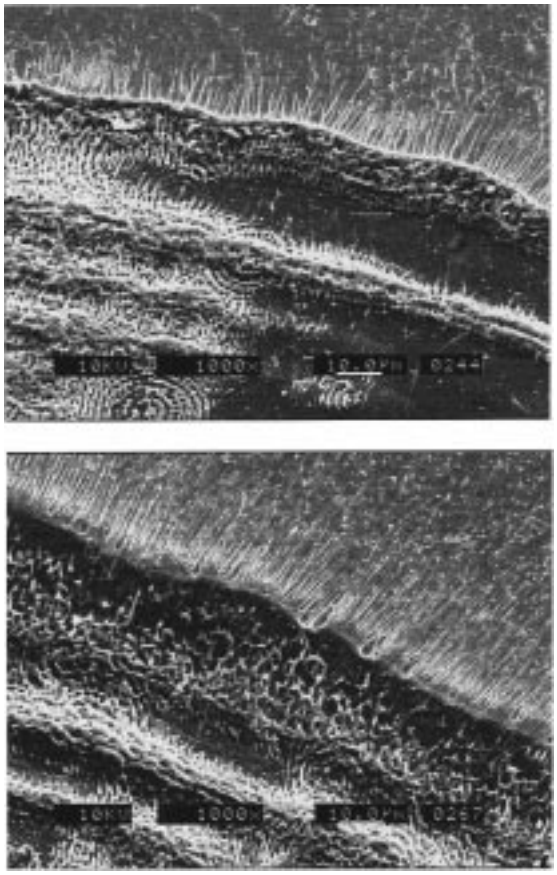

Figure 7. SEM micrographs of PMMA-IR (top) and PMMA-IR/UV (bottom) irradiated at 1064 nm (100 ps, 1.5 J/cm^2).

PMMA-UV. Irradiation at 266 nm (with Picosecond and Nanosecond Pulses). The DMA-doped PMMA-UV sample exhibits surface swelling when irradiated at 266 nm with nanosecond or picosecond pulses. At some parts of the swollen area the surface is burst and reveals a porous structure, while at higher fluences the area looks spongy (Figure 9). The swelling is more distinct for picosecond pulses. From the heights determined with a profiler and shown in Figure 10, a threshold

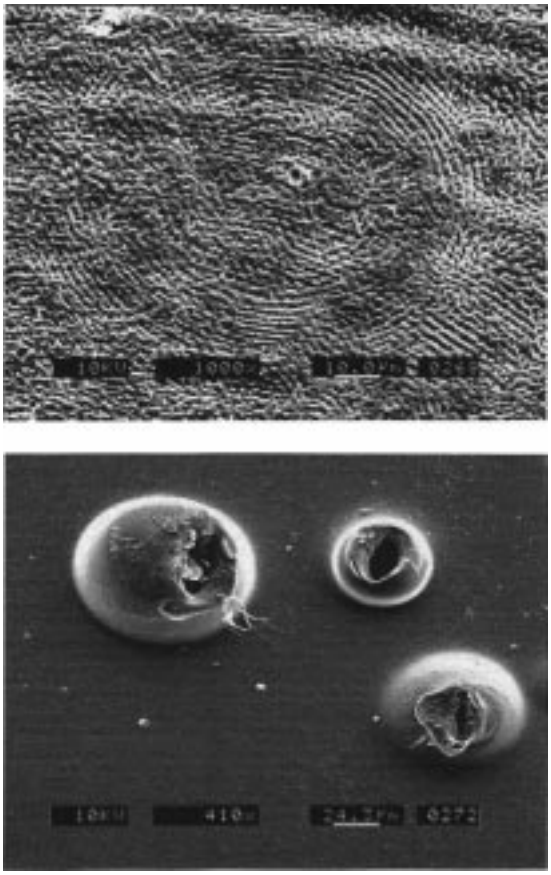

Figure 8. SEM micrographs of PMMA-IR (top, single pulse) and PMMA-IR/UV (bottom, multiple pulses) irradiated at 1064 nm (100 ps, 1.5 J/cm^2).

fluence for surface swelling can be determined. For the lowest investigated fluence no swelling but surface roughening was detected.

For nanosecond irradiation the swelling/etching is too irregular to determine definite values with the profiler. Even with multiple pulses of picosecond or nanosecond duration, no clean etching could be achieved; larger pieces of debris are redeposited in and around the irradiated area. The edges of the craters are shown in Figure 11. An interesting detail is also exhibited in Figure 11; in contrast to the fine fibrous debris that is found in the other samples after IR irradiation at similar fluences, the debris after irradiation at 266 nm has a perfect spherical shape. The surface of this spheres is very smooth, and the diameters are up to 5 μm. When results from the two pulse lengths employed are compared, picosecond irradiation appears to produce spheres with larger diameters.

Discussion

Triazene Copolyesters. The comparison of the experiments at 266 and 1064 nm can be used to discuss the mechanism of ablation. Linear absorption coefficients are not informative for this purpose, since the ablation behavior is governed by the effective absorption behaviors given in the Results. A variety of effects are contributing toward effective absorption, as has been discussed in detail elsewhere (cf. ref 14 and references given therein).

For the triazene copolyesters the results of ablation at 266 nm resemble the findings of experiments at 308 nm. In these investigation 35−50% triazene units were found to be the optimum concentration with respect to the achieved quality of the micropattern.[14] With this chromophore concentration neither redeposited debris nor bubble formation was observed. This tendency could be confirmed for 266 nm irradiation. Figure 1 shows that both irradiation wavelengths (266 and 308 nm) are exciting the chromophor within the same absorption band, in detail the $\pi \rightarrow \pi^*$ transition of the triazene group. The absorption coefficient at 266 nm is lower compared to the absorption at 308 nm. The triazene groups represent both the chromophoric moieties and at the same time the sites of photolability. This introduces a defined decomposition pattern into the polymer chains, resulting in high-resolution etching with no redeposited material.

The fact that the etching rates at 266 nm are decreasing with shorter pulse lengths at the same fluence can be explained by losses due to dynamic absorption and multiphoton absorption, which is important at low fluences.[15−17] Excited states can also absorb at sufficiently high photon densities, but since these states have a lifetime in the picosecond range, this effect does not play a role if pulses of nanosecond duration are used at comparable fluences.

The lower ablation rate for the higher concentration of the absorbing chromophore, which results in a higher absorption coefficient, is expected for nanosecond ablation. In investigations of systems, doped either with monomers or polymers, the threshold fluence and the limiting etch rates were found to be strongly dependent on the absorption coefficient, i.e., the dopant concentration.[18−21] High dopant concentrations result in lower threshold fluences and lower ablation rates.

In contrast, for the ablation at 308 nm at high fluences no strong dependence of the parameters on the concentration was found. This is probably due to a change of the ablation mechanism at high fluences, e.g., plume absorption or dynamic absorption behavior. For similar triazene polymers bleaching of the chromophore during the pulse has been identified as an important feature.[22] The quality of the etched structure can be improved by increasing the triazene content. With a higher amount of the photolabile chromophore, the mechanism is dominated by photochemical features.

This conclusion is supported by the fact that the attempt to induce photothermal ablation in the IR by the molecular heater IR-165 was unsuccessful. Instead, in single-pulse experiments the material was mainly swollen, and just in some parts enough pressure was built up to rupture the surface layers. Obviously, the released thermal energy was not sufficient to break the polymer chain into small fragments that leave the matrix. Multiple pulses delivered enough energy to etch material, but here as well, the fibrous debris shows that the fragmentation was incomplete. The difference of single-pulse irradiation resides in the fact that with the first pulse the material is modified so that new absorption sites can be created (e.g., by carbonization). The polymer starts to decompose at 225 °C; thermogravimetric experiments showed that the first step is the extrusion of the structural unit $-N{=}N-N(CH_3)C_2H_4N(CH_3)-N{=}N-$.[23] Thus, it is conceivable that cross-links are formed within the remaining polymer, and a thermally more stable compound results. It also has to be taken into account that, since the laser provides heating rates up to 1 billion °C per second, reaction rates cannot keep up with the temperature increase, the material is superheated, and the chemistry can be quite different from that usually obtained at thermal equilibrium.

Doped PMMA Films. A pronounced difference was found for the doped PMMA films. Effective etching can be achieved with IR picosecond irradiation. One reason might be that the repetition units are much smaller for PMMA than for the copolyester and that PMMA is known to start an unzipping

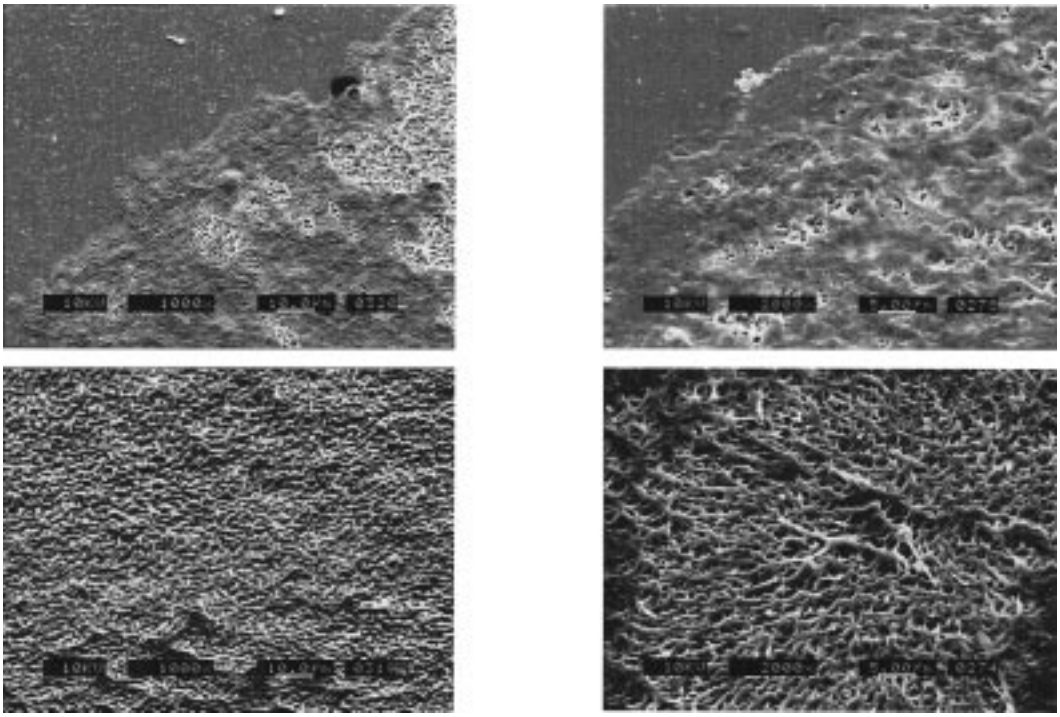

Figure 9. SEM micrographs of PMMA-UV after irradiation at 266 nm with 6 ns (top left, 0.22 mJ/cm^2; bottom, 0.49 mJ/cm^2) or 60 ps (top right, 0.26 mJ/cm^2; bottom, 0.53 mJ/cm^2) pulses.

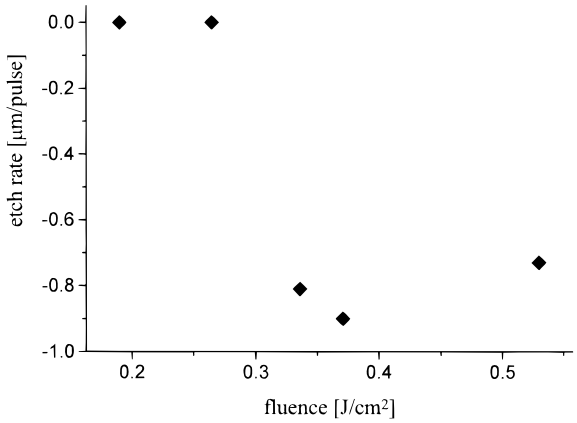

Figure 10. Etch rates, i.e., the swelling, of PMMA-UV after irradiation at 266 nm (60 ps) as a function of the fluence.

process after reaching its ceiling temperature. After depolymerization there is enough excess energy so that the fragments can leave the matrix.

Lee and co-workers[8] investigated PMMA doped with 15 wt % IR-165 under ablative conditions (1064 nm, 100 ns) with conventional and optical calorimetry. They introduced a two-step model: the first step includes the rapid pyrolytic formation of reactive species initiating chain reactions, which is followed by a temperature-dependent depolymerization process. Significant decomposition was found to start at 300 °C, while at threshold fluences the peak surface temperature is around 600 °C. A further increase in intensity leads to a limiting temperature of 715 °C. The fluence was given to be in the range of mJ/cm^2. The determined threshold fluence of about 70 mJ/cm^2 for 100 ns pulses is much smaller than the fluences determined in our case. The reason for this discrepancy is that they used as criterion the decomposed fraction determined by calorimetry while we tried to detect the ablated depth with a profiler, which is a much less sensitive method.

For high-resolution structuring by laser ablation, the effective

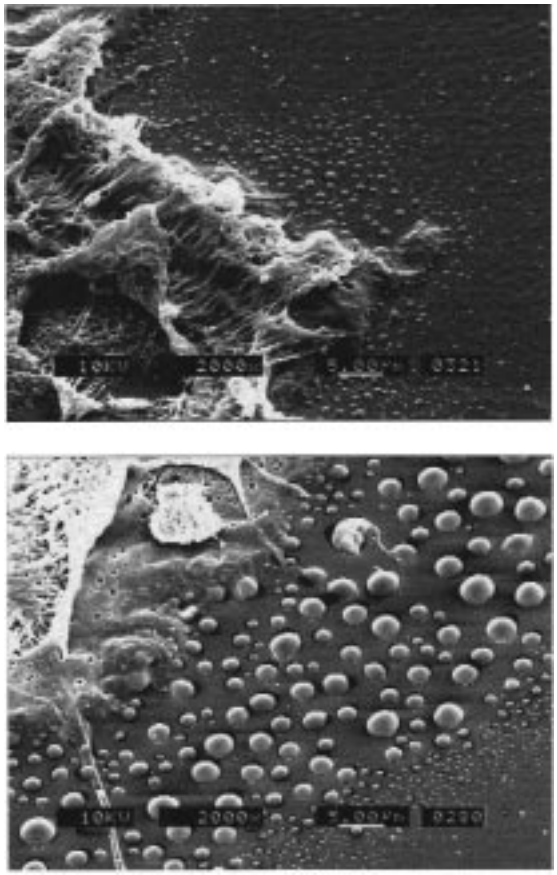

Figure 11. SEM micrograph showing the spherically shaped debris that is redeposited at the crater edge after repetitive irradiation of PMMA-UV at 266 nm (top, 6 ns; bottom, 60 ps).

removing of surface layers is most important. From three-dimensional imaging by the profiler we know that the surface is partly etched for nanosecond pulses (meaning decomposition), but the roughening is too strong to determine the etch depths

reliably, which does not exclude, of course, the observation that substantial fractions are already decomposed. The SEM micrographs in Figure 6 show that the decomposed material of the first pulse can effectively be removed by successive pulses.

In contrast, with picosecond pulses, etching with single pulses could be achieved in the investigated fluence range (Figure 7). The partly spongy, partly cleanly etched surface in the top left of Figure 7 is most probably due to the inhomogeneous beam profile. With higher fluences the molten material is removed completely, while at lower fluence some decomposed material remains. The comparison leads to the conclusion that not only the total absorbed energy but also the pulse length and accordingly the intensity play an important role in the photothermal ablation mechanism. This was stated before for strongly absorbing and thermally well-conducting materials such as metals.[24,25] Obviously, the energy loss to the bulk is less important in the case of polymers, since the thermal conductivity is much smaller.

The dynamics of the optical point heater IR-165 in a PMMA matrix were studied by Wen and co-workers for a pulse length of 100 ps.[26] Since the absorption recovery time is only about 0.2 ps and the saturation intensity is as high as 8.9 GW/cm^2, ultrafast temperature jumps are possible. Multiphonon pumping of the matrix was identified as an important process on the 0.1−100 ps time scale. Since it is known that multiphonon up-pumping plays a crucial role in the activation of molecular vibrations in solid-state thermochemical reactions and also in shock-induced detonation of energetic material,[27,28] it should also be essential in the ablation procedure and may therefore be responsible for the difference between nanosecond and picosecond ablation.

The result that the addition of DMA is not improving the ablation, in detail does not increase the etch rates (Figure 5), means that the gaseous decomposition products are not supporting the material removal. In the case of a mechanism that involves the volume increase by decomposition, we would expect a significant contribution to the etch rate even in the IR, since the induced temperatures are higher than the decomposition temperature of DMA.

Fujiwara et al.[10] found in a recent investigation that the main contribution of DMA to the ablation of PMMA films at 248 nm proceeds via heat generation and thus a photothermal mechanism. DMA is decomposed to a ketene in a first step and then generates a rapid temperature increase by cyclic many-photon heat generation (up to 10 cycles are completed by one dopant molecule during a laser pulse of 30 ns pulse width). Accordingly, ablation proceeds via a thermal mechanism and there is little or no contribution by photodecomposition. Consequently, if we introduce thermal decomposition of DMA at 1064 nm, no further heat generation by cyclic absorption can take place and our findings are in agreement with these studies. A similar photothermal mechanism of dopant-sensitized ablation was reported by Arnold and Scaiano for irradiation of PMMA doped with 1,1,3,3-tetraphenylacetone at 266 nm.[3]

The only hint of an assistance to the etching process by the nitrogen release of decomposed DMA is the occurrence of burst bubbles at repetitively irradiated areas (Figure 8, bottom). These bubbles are not detected in samples doped only with IR-165 (Figure 8, top). Maybe these craters originate from an inhomogeneous distribution of the dopant molecules, thus creating a high pressure locally.

The appearance of the concentrical, equidistant ring pattern is not yet understood. These patterns are only found in samples of doped PMMA films after irradiation with 1064 nm and a pulse duration of 100 ps (Figure 7, top; Figure 8, top). A possible explanation would be diffraction and interference of the beam at crystallites in the otherwise amorphous PMMA film.

Assuming the cyclic many-photon absorption, we can also explain the results of the 266 nm irradiation of PMMA-UV. With picosecond irradiation we observe only swelling in the investigated fluence range (the cyclic mechanism will be much less effective in the picosecond time scale because fewer photons can be used). For the nanosecond irradiation an extreme roughening of the surface is detected. This roughening can be explained by a combination of swelling and etching: while at the topmost layers the fragments possess enough energy to leave the surface, the underlying parts lack it, and thus swelling occurs.

The swelling that follows picosecond irradiation can thus be regarded as an incomplete fragmentation and ejection. Since comparable fluences were applied, it can be concluded that less energy was incorporated into the matrix. The model of cyclic many-photon absorption backs this interpretation because fewer cycles of absorption and relaxation can be completed during a picosecond pulse and consequently less thermal energy is coupled into the matrix.

An additional feature of the UV ablation of DMA-doped PMMA is the occurrence of the rather large spherical shaped debris in contrast to the fibrous residue usually observed at the edge of the craters. It appears that liquid droplets with a low viscosity have been ejected that exhibit a high interfacial tension toward the bulky material at the walls. This could also indicate that the ejected material at different temperatures from IR or UV heating is different, e.g., of different molecular weight. The arrangement and shape of the droplets is compatible with condensation (nucleation and growth) from the gas phase.

Conclusions

Several experiments were performed to compare the ablation behavior in the IR and UV of a doped standard polymer, PMMA, and a specially designed photopolymer to obtain hints on the underlying mechanism, namely, photochemical vs photothermal.

From the unsuccessful attempt to induce ablation in the IR by doping the triazene copolyester with an optical molecular heater we concluded that the etching process in the UV for this type of polymer should mainly be governed by a photochemical process. Photons are absorbed by the triazene chromophores that function as design fracture points in the main chain and thus enable clean etching with high resolution. This is true for irradiation at 266 and 308 nm exciting the same $\pi \rightarrow \pi^*$ transition. In the case of the photothermal process via the IR dye, only swelling was achieved; after delivery of several pulses undefined craters with a lot of debris and thermally damaged walls were produced. This is explained by possible cross-linking of large polymer fragments that remain in the matrix after the first step of thermal decomposition, namely, the extrusion of the functional triazene group.

In contrast, since the thermal decomposition of PMMA involves an unzipping depolymerization process that finally leads to small monomeric units, etching of doped PMMA films in the near-IR is possible. High-intensity irradiation with picosecond pulses leads to defined etching, while nanosecond pulses result in strong surface roughening, which was difficult to investigate with the profiler.

The comparison of the etch rates of PMMA doped with IR-165 and additionally with DMA irradiated at 1064 nm showed that there is no auxiliary effect of the DMA. This is consistent with a current theory that explained the sensitizing effect of

DMA in the UV through simple heating via cyclic many-photon absorption and not via photodecomposition.[10]

The results of UV-induced ablation of PMMA doped with DMA can also be explained by this photothermal model. The swelling, which is more distinct for picosecond irradiation than for nanosecond irradiation at the same fluence, can be seen as incomplete fragmentation and ejection of decomposed material. This is due to a lack of excess energy, since fewer cycles of photon absorption and relaxation can be completed during the shorter pulse duration.

In addition to these insights into the ablation mechanism, a practical conclusion can be drawn: it seems to be inevitable to incorporate the absorbing chromophore into the main chain of the polymer if the quality of the achieved structure is of relevance. In other cases thermal damage will always impair the achieved pattern.

References and Notes

(1) Suzuki, K.; Matsuda, M.; Ogino, T.; Hayashi, N.; Terabayashi, T.; Amemiya, K. *SPIE Proc.* **1997**, *2992*, 98.
(2) Fukumura, H.; Masuhara, H. *Chem. Phys. Lett*. **1994**, *221*, 373.
(3) Arnold, B.; Scaiano, J. *Macromolecules* **1992**, *25*, 1582.
(4) Wen, X.; Hare, D.; Dlott, D. *Appl. Phys. Lett*. **1994**, *64*, 184.
(5) Srinivasan, R.; Braren, B. *Appl. Phys. A* **1988**, *45*, 289.
(6) Bolle, M.; Luther, K.; Troe, J.; Ihlemann, J.; Gerhardt, H. *Appl. Surf. Sci*. **1990**, *46*, 279.
(7) Lippert, Th.; Wokaun, A.; Stebani, J.; Nuyken, O.; Ihlemann, J. *Angew. Makromol. Chem.* **1993**, *213*, 127.
(8) Lee, I.; Wen, X.; Tolbert, W.; Dlott, D.; Doxtader, M.; Arnold, D. *J. Appl. Phys*. **1992**, *72*, 2440.
(9) Willson, C.; Miller, R.; McKean, D. *Proc. SPIE Adv. Resist Technol. Process.* **1987**, *4*, 771.
(10) Fujiwara, H.; Nakajima, Y.; Fukumura, H.; Masuhara, H. *J. Phys. Chem.* **1995**, *99*, 11481.
(11) Nuyken, O.; Dahn, U. *J. Polym. Sci*., Part A: Polym. Chem. **1997**, *35*, 3017.
(12) Srinivasan, R.; Braren, B. *Chem. Rev.* **1989**, *89*, 1303.
(13) Srinivasan, R.; Braren, B.; Casey, K. *J. Appl. Phys*. **1990**, *68*, 1842.
(14) Hahn, Ch.; Kunz, Th.; Dahn, U.; Nuyken, O.; Wokaun, A. *Appl. Surf. Sci.* **1998**, *127*−*129*, 899.
(15) Sutcliff, E.; Srinivasan, R. *J. Appl. Phys*. **1986**, *60*, 3315.
(16) Kalontarov, L. *Philos. Mag. Lett.* **1991**, *63*, 289.
(17) Küper, S.; Stuke, M. *Appl. Phys. B* **1987**, *44*, 199.
(18) Lippert, T.; Wokaun, A.; Stebani, J.; Nuyken, O.; Ihlemann, J. *Angew. Makromol. Chem.*. **1993**, *213*, 127.
(19) Masuhara, H.; Hiraoka, H.; Domem, K. *Macromolecules* **1987**, *20*, 452.
(20) D'Couto, G.; Babu, S.; Egitto, F.; Davis, C. *J. Appl. Phys*. **1993**, *74*, 5972.
(21) Egitto, F.; Davis, C. *Appl. Phys. B* **1992**, *55*, 488.
(22) Lippert, T.; Bennett, L.; Nakamura, T.; Niino, H.; Ouchi, A.; Yabe, A. *Appl. Phys. A* **1996**, *63*, 257.
(23) Dahn, U. Thesis, TU München, Munich, Germany 1997.
(24) Preuss, S.; Matthias, E.; Stuke, M. *Appl. Phys. A* **1994**, *59*, 79.
(25) Tolbert, W.; Lee, I.; Wen, X.; Dlott, D. *J. Imaging Sci. Technol*. **1993**, *97*, 485.
(26) Wen, X.; Tolbert, W.; Dlott, D. *Chem. Phys. Lett.* **1992**, *192*, 315.
(27) Dlott, D.; Fayer, M. *J. Chem. Phys.* **1990**, *92*, 3798.
(28) Kim, H.; Dlott, D. *J. Chem. Phys*. **1990**, *93*, 6395.